AD-A056 431 ARMY MISSILE RESEARCH ANC DEVELOPMENT COMMAND REDSTO--ETC F/G 20/14
FOG AND HAZE IN EUROPE AND THEIR EFFECTS ON PERFORMANCE OF ELEC--ETC(U)
JUN 78 O M ESSENWANGER, D A STEWART

UNCLASSIFIED NL

| OF |
AD
A056431

END
DATE
FILMED
8 -78
DDC

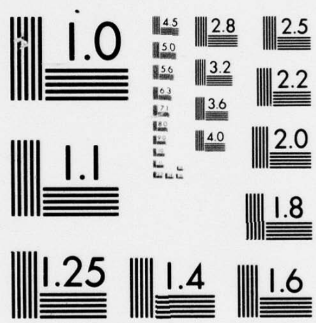

MICROCOPY RESOLUTION TEST CHART
NATIONAL BUREAU OF STANDARDS-1963-A

*ESSENWANGER and STEWART

LEVEL II

(12) 15p.

AD A056431

AD No.
DDC FILE COPY

DDC
RECEIVED
JUL 10 1978
D

(11) JUN 1978

(6) FOG AND HAZE IN EUROPE AND THEIR EFFECTS ON PERFORMANCE OF ELECTRO-OPTICAL SYSTEMS. (U)

(10) *OSKAR M. ESSENWANGER, ~~DR.~~, and DORATHY A. STEWART, DR.
~~US ARMY MISSILE RESEARCH AND DEVELOPMENT~~ COMMAND
REDSTONE ARSENAL, ALABAMA 35809

INTRODUCTION

It is well known that aerosols which cause poor visibility affect infrared and submillimeter wave propagation, and water vapor causes significant additional attenuation of the near-millimeter wavelengths. Direct estimates of climatological probabilities for the degrading performance are difficult to obtain. These probabilities require the knowledge of the liquid water content and the drop-size distribution, and neither quantity is observed on a routine basis. In the past the liquid water content was often assumed to be a unique function of the visibility. This postulation is erroneous because the relationship between visibility and liquid water content depends upon the drop-size distribution.

The second quantity, drop-size distribution, is even more deficient because information is available only from sporadic measurements made during specific research projects of insufficient duration to develop a systematic climatology of drop-size distributions. Available information in the literature has recently been summarized by Stewart (12). There are large variations, but on the average fogs caused primarily by radiational cooling (radiation fogs) have smaller drops than other fogs.

We have attempted to develop a propagation climatology by inference from the frequency of occurrence of different types of fog. The methodology is presented in detail in the next 3 sections. The analysis resulted in the estimation of average attenuations of different wavelengths by fogs in Central Europe. Attenuation of 1250-μm energy is always less than attenuation of 870 μm in fog. Average

78 06 12 024

393 169

attenuation of 870 μm in dense fogs is much less than attenuation of 10.6 μm in all seasons. In summer 10.6 μm penetrates light fog better than 870 μm, but 10.6 μm penetrates less well than 1250 μm.

Before the details of our research effort are discussed, the occurrence of poor visibility in Central Europe will be reviewed. It is known that fog has a distinct diurnal variation with the highest chances of occurrence in the early morning hours. Ten stations were selected from Central Europe, and the frequency of fog (visibility $\leq$ 1 km) was established. The result is depicted in Figures 1 and 2. We learn from Figure 1 that for most stations fall is the worst season having the highest amount of morning fogs up to 25% of the time, and winter is next. Had we included monthly results the frequency for the worst month at some stations would have been more than 30% of the early morning hours.

Fuerstenfeldbruck has been selected to illustrate the duration of fogs. As disclosed in Figure 2 one case with over 120 hours of consecutive fog existed, and fog was present in the morning hours on 13 consecutive days. Consequently, poor visibility occurs frequently enough to warrant the consideration of the degrading effect on electro-optical propagation. Further details are given by Essenwanger (2, 3, 4) and Essenwanger and Stewart (6).

THE FOG CLASSIFICATION MODEL

Because average drop sizes are usually smaller in radiation fog than in other fogs, electromagnetic energy with wavelengths in the middle infrared and longer should penetrate radiation fog better. Recent measurements published in the meteorological literature (e.g., Mészaros, 9, and Pilié et al., 11) contradict the widespread belief that fogs remote from coastal areas can be assumed to be pure radiation fogs. However, no probabilities of occurrence are available.

Unfortunately, fog is not classified by the observer at the time of measurement, and a detailed analysis of individual fog cases is tedious and time consuming. Consequently, the authors sought a computerized method which could be efficiently applied to large data collections. It is difficult to develop a computer model which separates all known types of fog because most fogs are mixtures of processes, and some radiative cooling occurs in nearly all of them. Therefore our goal was the separation of fogs into primary groups: those caused predominantly by radiational cooling and all other types. Although the individual fog may be a borderline case and be placed into the wrong group, these cases should balance out in a statistical sense.

FIG. 1. FREQUENCY OF VISIBILITY $\leq$ 1KM (SEASONS)

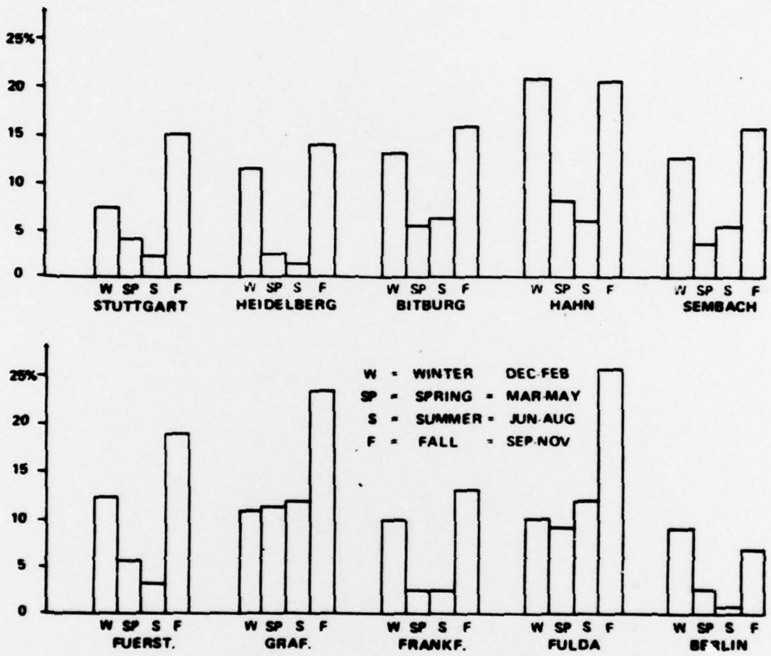

FIG. 2. MAXIMUM DURATION OF VISIBILITY $\leq$ 1KM

FUERSTENFELDBRUCK

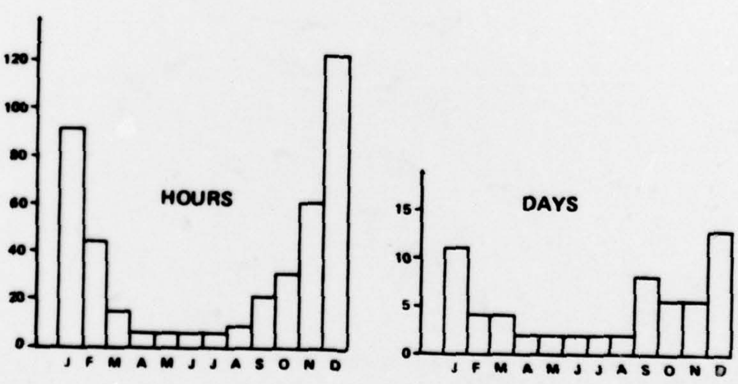

Figure 3 delineates the computer processing of the data at an individual station with observations in synoptic code form. The flow chart should be self-explanatory, and the grouping is described in detail in a forthcoming report by Essenwanger (5). The model is applicable to morning fogs, and is based on precipitation, cloud and temperature behavior in fog processes. A clear or partly cloudy night leads to radiation fog (class 11-13) while precipitation and an overcast sky imply the presence of predominantly non-radiative types (class 6-8). Class 9 remains a mixture of both but the data cannot be separated without a considerable increase in computer costs. A splitting of this class in half is very cost effective, and this simple rule has no significant impact on the final outcome. The model was robust to reasonable changes in cloud conditions. Table 1 provides an excerpt from the detailed tables in the report by Essenwanger (5), and illustrates the grouping of fogs for 10 stations in Central Europe.

The reasonable functioning of the fog classification model is supported by results depicted in Figures 4 and 5. These show the cumulative frequency of wind speeds and dew points by fog groups during fall and winter. As expected, radiation fogs display a lower wind speed and dew point than non-radiation fogs. More details can be found in Essenwanger (5).

Table 1. Grouping of Fog From the Model in Figure 3 (in ‰ of Fog).

	Fall				Winter				Spring			
	NR ‰	M ‰	R ‰	N	NR ‰	M ‰	R ‰	N	NR ‰	M ‰	R ‰	N
Stuttgart	73	147	780	2234	154	256	590	2196	99	198	703	2208
Heidelberg	154	201	645	1546	246	347	407	1561	209	116	675	1623
Bitburg	206	206	588	1661	461	262	277	1654	180	157	663	1666
Hahn	245	315	440	1623	419	353	228	1292	403	258	339	1555
Sembach	114	127	759	1559	305	288	407	1499	64	149	787	1507
Fuerstenfeldbr.	218	243	539	1061	243	421	336	993	161	53	786	1081
Grafenwoehr	92	172	736	969	421	228	351	933	108	108	784	973
Frankfurt	268	271	461	2273	363	381	256	2192	241	241	518	2206
Fulda	246	0	754	799	-	-	-	-	125	83	792	840
Berlin	215	321	464	2275	346	318	336	2197	143	224	633	2269

NR = non-radiation fog (class 6-8). M = mixture (class 9).
R = radiation fog (class 11-13). N = total data base in days.

FIG. 3.

FOG CLASSIFICATION MODEL

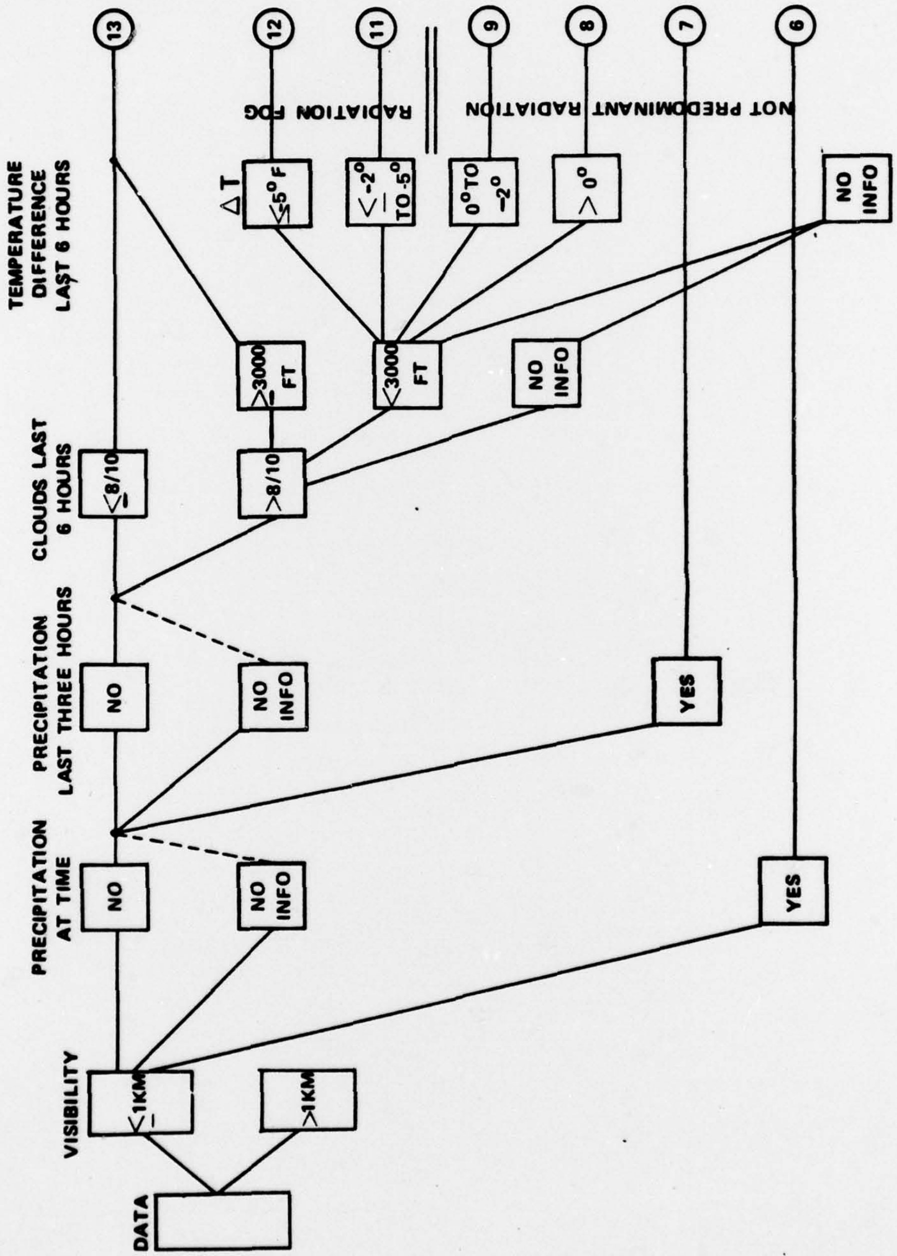

FIG. 4. WIND SPEED IN GERMAN FOGS

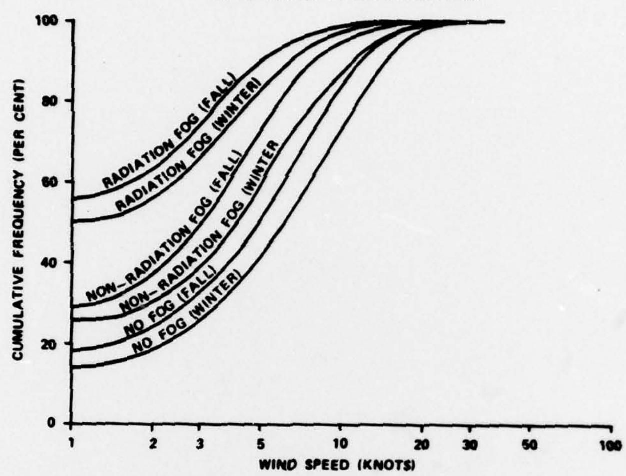

FIG. 5. DEW POINTS IN GERMAN FOGS

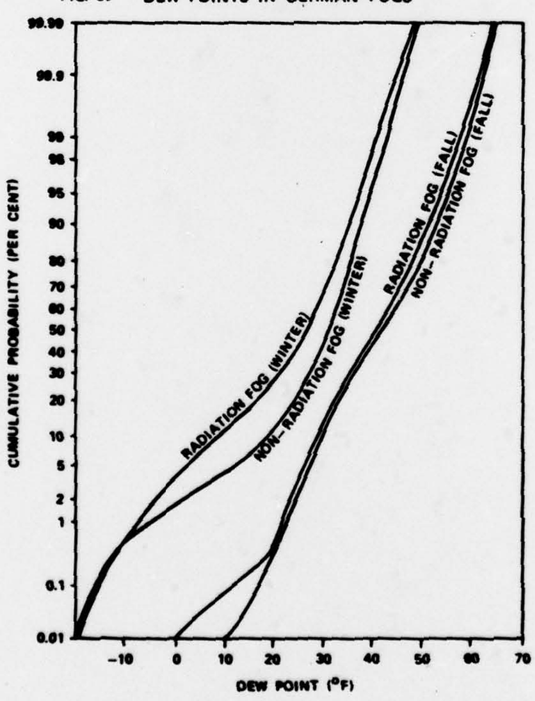

THEORETICAL COMPUTATIONS

Extinction of electromagnetic energy by fog droplets depends upon the wavelength of the energy, the complex index of refraction of the drops for that wavelength, and the drop-size distribution. We chose to compute attenuations for the wavelengths of 0.55, 10.6, 870, and 1250 μm. The complex index of refraction of water for 0.55 μm was taken from Hale and Querry (7), and the value for 10.6 μm was interpolated from a table in the same article. Davies et al. (1) made measurements from which the index of refraction of water for 1250 μm could be computed, and the value for 870 μm was interpolated from their data. The computational procedure for obtaining theoretical attenuations based on Mie (10) theory is outlined by Stewart (12). She made an extensive literature survey, and her report lists the references for the drop-size distributions used in this study.

Figures 6-9 illustrate some of the results of our computations. Figure 6 is a plot of visibility as a function of attenuation at 10.6 μm, and one can readily see that there is a great deal of scatter in the data. An attenuation of 50 dB/km at 10.6 μm can be associated with visibilities over 300 m or considerably less than 100 m. Figure 7 depicts the relation of visible and 1250-μm attenuations, and these data contain even more scatter than the data in Figure 6. Figure 8 shows that 10.6-μm attenuation by fog droplets is more closely correlated with 1250-μm attenuation than it is with visible attenuation. Figure 9 contains a plot of 870 μm attenuation versus 1250-μm attenuation, and it is obvious that these attenuations are very closely correlated.

The data in Figures 6-9 were examined individually to determine which fogs could be classified as radiation or non-radiation fogs. Table 2 contains the expected mean attenuations of 10.6, 870, and 1250 μm by fog drops for three different visibilities.

Water vapor is another source of extinction of infrared and near-millimeter wavelengths. McCoy et al. (8) gave a formula for computing attenuation of the 10.6-μm wavelength by water vapor. Webster (13) developed a procedure for computing water vapor attenuation near 1 mm. The attenuation by water vapor depends primarily upon the amount of water vapor and the temperature, but there is also a slight pressure dependence. Figure 10 displays the cumulative frequency distribution of attenuation of 870 μm by water vapor for radiation and non-radiation fogs in fall and winter in Germany.

FIG. 6. PLOT OF VISIBILITY VERSUS ATTENUATION AT 10.6–μm

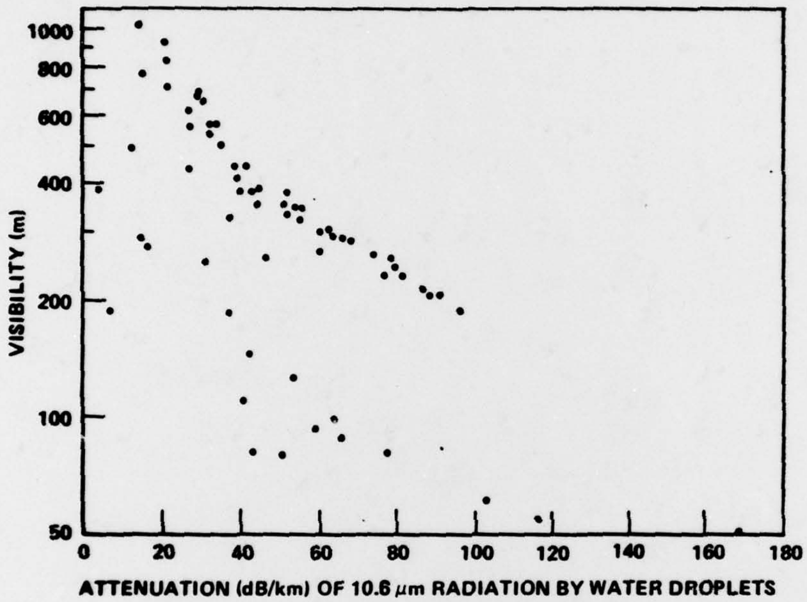

FIG. 7. COMPARISON OF ATTENUATIONS OF 1250- μm AND 0.55–μm WAVELENGTHS BY FOG DROPLETS

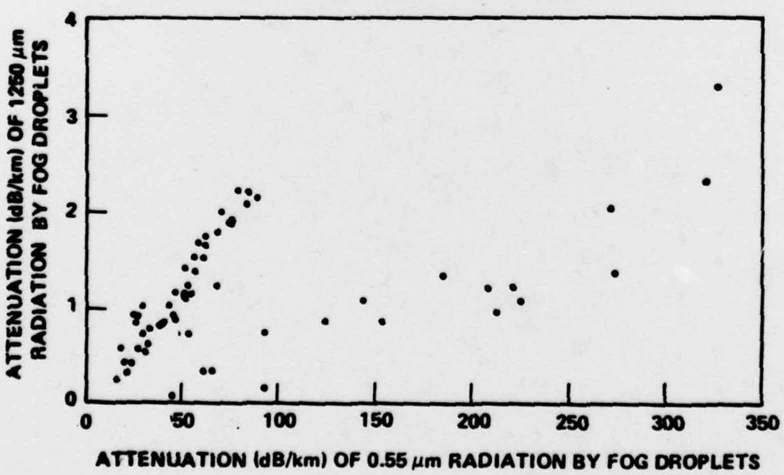

FIG. 8. COMPARISON OF ATTENUATIONS OF 1250-μm AND 10.6-μm WAVELENGTHS BY FOG DROPLETS

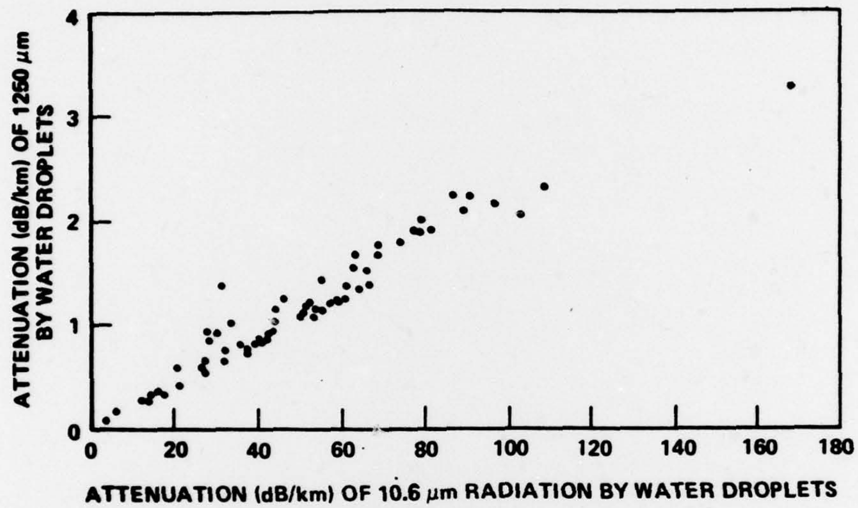

FIG. 9. COMPARISON OF ATTENUATIONS OF 1250-μm AND 870-μm WAVELENGTHS BY FOG DROPLETS

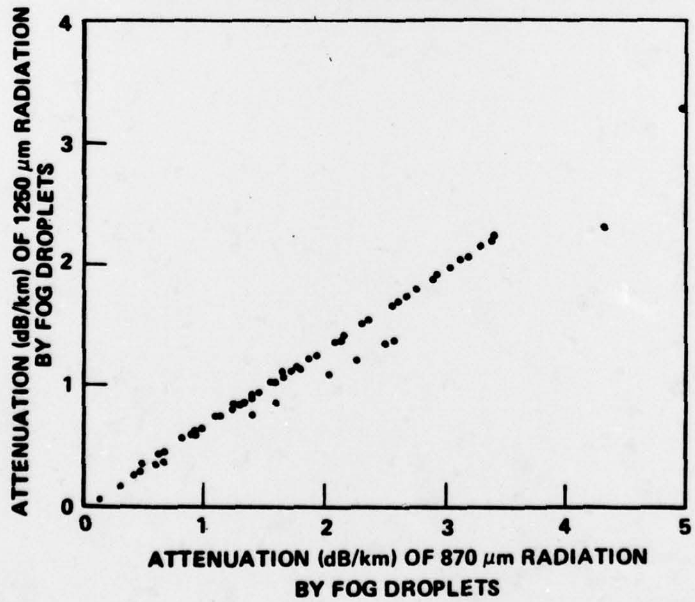

FIG. 10. ATTENUATION OF 870 μm BY WATER VAPOR IN GERMAN FOGS

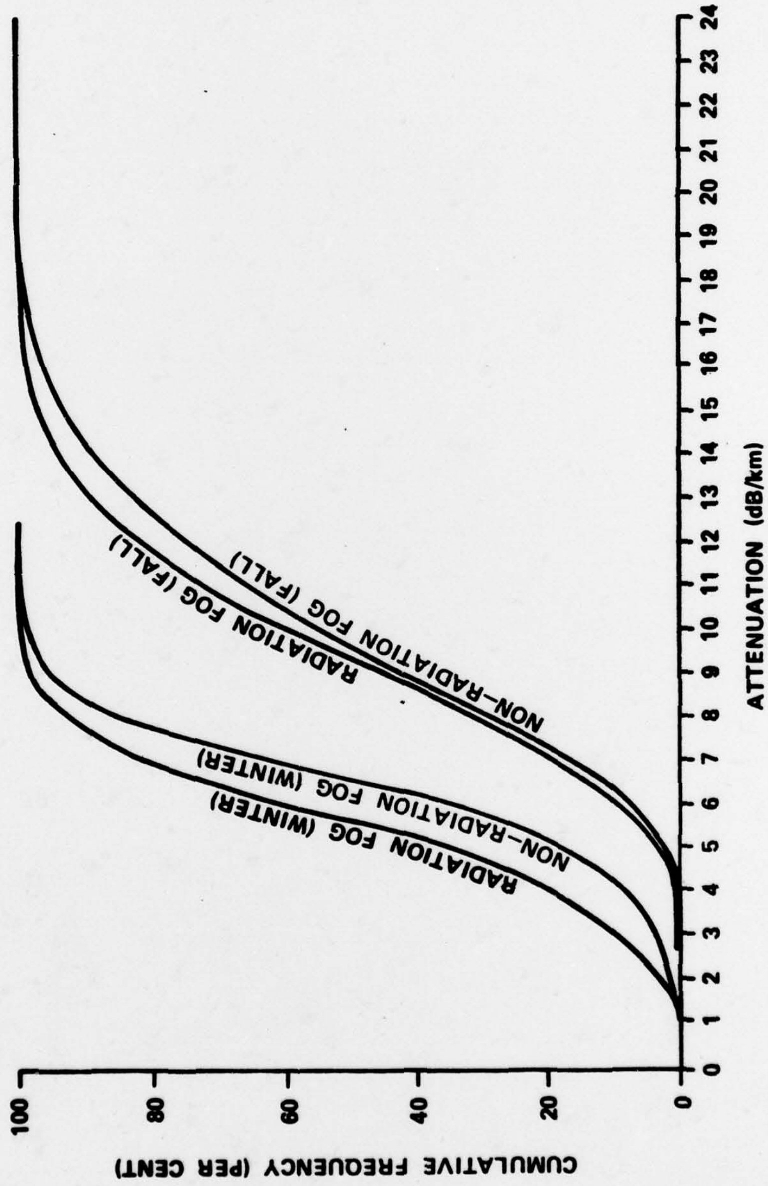

Table 2. Expected Mean Attenuation (dB/km) by Fog Droplets.

	Visibility		
	1000m	400m	200m
0.55 μm	16.99	42.47	84.95
10.6 μm, radiation fog	5.95	14.87	29.73
10.6 μm, non-radiation fog	14.78	36.95	73.91
870 μm, radiation fog	0.21	0.52	1.04
870 μm, non-radiation fog	0.54	1.34	2.68
1250 μm, radiation fog	0.12	0.31	0.62
1250 μm, non-radiation fog	0.35	0.87	1.74

PROPAGATION CLIMATOLOGY

From the above theoretical framework and climatological information one can infer climatological attenuation characteristics for fogs in Europe. The mean attenuations by radiation and non-radiation fog droplets in Table 2 were weighted according to the number of fog cases in Table 3. Table 4 contains the mean attenuations by water vapor. These have been weighted according to the number of fog cases in Table 3 and added to the mean attenuations by fog droplets to obtain the mean total attenuations in Table 5. One sees that 1250 μm penetrates fog better than both 10.6 μm and 870 μm in all seasons and for all visibilities. This occurs because attenuations by both water vapor and fog drops are small at 1250 μm. At 10.6 μm attenuation by water vapor is always small but attenuation by fog drops may be quite large, especially in non-radiation fogs which typically have larger drops than radiation fogs. In winter when about half the fogs are non-radiation fogs, average attenuation of 10.6 μm is considerably larger than attenuation of 870 μm for all visibilities. In summer water vapor attenuation causes average 870-μm attenuation to be larger than 10.6-μm attenuation in light fogs, but 870-μm attenuation is less than 10.6-μm attenuation in dense fogs. In spring and fall 10.6 μm and 870 μm have comparable attenuations in light fogs, but 870 μm is attenuated less in heavy fogs. From 0600 to 0800 Greenwich Mean Time 64 per cent of fogs have visibilities less than 500 m in spring and 75 per cent in fall.

Table 3. Number of Cases of Fog From Ten German Stations at 0600 Greenwich Mean Time.

Type of Fog	Winter	Spring	Summer	Fall
Radiation	672 (49.8%)	477 (71.9%)	456 (77.8%)	1591 (71.3%)
Non-Radiation	677 (50.2%)	186 (28.1%)	130 (22.2%)	641 (28.7%)

Table 4. Mean Attenuation (dB/km) by Water Vapor in Germany at 0600 Greenwich Mean Time.

	Radiation Fog			Non-Radiation Fog		
	10.6 μm	870 μm	1250 μm	10.6 μm	870 μm	1250 μm
Winter	0.11	5.61	1.74	0.14	6.63	2.06
Spring	0.21	8.16	2.54	0.25	9.06	2.82
Summer	0.50	13.45	4.21	0.64	15.38	4.82
Fall	0.29	9.82	3.06	0.32	10.26	3.20

Table 5. Expected Mean Attenuation (dB/km) in German Fogs at 0600 Greenwich Mean Time.

Season	Wavelength (micrometers)	Visibility 1000m	400m	200m
Dec - Feb	10.6	10.5	26.1	52.0
	870	6.5	7.1	8.0
	1250	2.1	2.5	3.1
Mar - May	10.6	8.6	21.3	42.3
	870	8.7	9.2	9.9
	1250	2.8	3.1	3.6
Jun - Aug	10.6	8.4	20.3	40.1
	870	14.2	14.6	15.3
	1250	4.5	4.8	5.2
Sep - Nov	10.6	8.8	21.5	42.7
	870	10.3	10.7	11.5
	1250	3.3	3.6	4.0

SUMMARY AND CONCLUSIONS

It is generally agreed that propagation of electromagnetic energy is affected by fog drops and water vapor, but climatological probabilities of attenuation do not exist except for the visible range which has wavelengths from about 0.4 to 0.7 μm. Unfortunately, attenuation in the visible portion of the spectrum does not uniquely determine attenuation of other wavelengths. The ratio of middle infrared attenuation to visible attenuation is determined mainly by the sizes of the drops in a fog because water vapor attenuation is small in the middle infrared and negligible in the visible. Water vapor is an important factor to be considered near one millimeter (see Table 4).

Average drop sizes depend primarily upon the meteorological processes which cause condensation. Fogs caused primarily by radiational cooling (radiation fogs) typically have smaller drop sizes than other fogs. Droplet sizes for fogs of each type vary widely with a large dispersion around the average. The curve of droplet size distribution for non-radiation fogs is shifted toward larger droplet size relative to the curve for radiation fog. Some overlapping area exists, but in principle the two frequency curves are significantly different for large data collectives.

In order to handle large amounts of data for a statistical analysis, we developed a computerized model for morning fogs in which the classification depends upon precipitation, cloud cover and temperature changes during the previous six hours. Data for several years from ten stations in Central Europe were examined. Theoretical mean attenuations of 10.6, 870, and 1250 μm by water drops were calculated from a large sample of drop-size distributions in the literature. The theoretical attenuations by water vapor were calculated from the actual observed water vapor distributions (see Fig. 10). The two longer wavelengths are in window regions with respect to attenuation by water vapor. Our data indicated that average water vapor content in radiation fogs was less than in non-radiation fog (see Fig. 4, Table 4).

Attenuation of 1250 μm in fog is less than attenuation of 870 μm and 10.6 μm in both light, moderate, and heavy fog in all seasons. The relationship between 870 μm and 10.6 μm is more complex. In a light fog with a large water vapor content the attenuation of 870 μm by water vapor may be so large that the total attenuation of drops plus water vapor is larger at 870 μm than at 10.6 μm. In moderate and heavy fogs attenuation of 10.6 μm by water drops usually causes 10.6 μm to be attenuated more than 870 μm. With visibilities

of 200 m or less even radiation fogs attenuate 10.6 µm by 30 dB/km or more, and non-radiation fogs have attenuations in excess of 70 dB/km. On the other hand the maximum attenuation of 870 µm by water vapor in our large data sample was 24 dB/km (see Fig. 10). One must add the attenuation by fog drops to obtain the total attenuation. Fog drops in an average non-radiation fog of 50 m visibility would have an attenuation of 11 dB/km. Therefore, even an extreme attenuation of 35 dB/km for 870 µm is less than the average attenuation of 10.6 µm for visibilities of 200 m or less. According to Essenwanger (5) 49 per cent of German fogs in fall have visibilities less than 200 m. In winter, spring, and summer the corresponding percents are 36, 37, and 41, respectively. Therefore, one must conclude from our data that a system operating at 870 µm penetrates most European fogs better than 10.6 µm.

ACKNOWLEDGMENTS

The authors wish to express their appreciation for the assistance by Mrs. Helen M. Boyd and Mr. Don McLain in establishing computer programs for the classification of fog. Mrs. Clara Brooks deserves our thanks for her careful typing of the manuscript.

REFERENCES

1. Davies, M., G. W. F. Pardoe, J. Chamberlain, and H. A. Gebbie, 1970: Submillimetre- and millimetre-wave absorptions of some polar and non-polar liquids measured by Fourier transform spectroscopy. Trans. Faraday Soc., 66, Part 2, 273-292.

2. Essenwanger, O. M., 1973: On the Duration of Widespread Fog and Low Ceiling in Central Europe and Some Aspects of Predictability. US Army Missile Command, Technical Report RR-73-9, 58 pp.

3. Essenwanger, O. M., 1973: On Spatial Distribution of Visibility and Clouds in Central Europe. US Army Missile Command, Technical Report RR-73-10, 63 pp.

4. Essenwanger, O. M., 1977: Estimation of Absolute Humidity During Morning Fog in Central Europe. US Army MIRADCOM, Technical Report TR-77-10, 22 pp.

5. Essenwanger, O. M., 1978: A Model of Fog Classification Applied to Central Europe. US Army MIRADCOM Technical Report (in preparation).

6. Essenwanger, O. M. and D. A. Stewart, 1976: Fog Climatology in Central Europe and Inferred Propagation Characteristics. Proceedings of the Optical-Submillimeter Atmospheric Propagation Conference sponsored by the Office of the Director, Defense Research and Engineering 6-9 December 1976, Vol. 1, Unclassified Papers, pp 165-179.

7. Hale, G. M. and M. R. Querry, 1973: Optical constants of water in the 200-nm to 200-μm wavelength region. Appl. Optics, 12, 555-563.

8. McCoy, J. H., D. B. Rensch, and R. K. Long, 1969: Water vapor continuum absorption of carbon dioxide laser radiation near 10 μ. Appl. Optics, 8, 1471-1478.

9. Mészaros, A., 1965: Concentration et Distribution Dimensionnelle des Gouttelettes de Brouillards Atmosphérique. J. Rech. Atmos., 2, 53-64.

10. Mie, G., 1908: Beiträge zur Optik Trüber Medien, Speziell Kolloidaler Metallösungen. Annalen der Physik, 25, fourth series, 377-445.

11. Pilié, R. J., E. J. Mack, W. C. Kocmond, C. W. Rogers, and W. J. Eadie, 1975: The life cycle of valley fog, Part I: micrometeorological characteristics. J. Appl. Meteor., 14, 347-363.

12. Stewart, D. A., 1977: Infrared and Submillimeter Extinction by Fog. US Army Missile R&D Command Technical Report TR-77-9, 51 pp.

13. Webster, D. W., 1973: Military Potential of the Extreme Infrared: Technology and Applications. Naval Weapons Center Report TP 5565. Catalogued under AD 915347.